NASA Technical Paper 2808

May 1988

Shape Sensitivity Analysis of Wing Static Aeroelastic Characteristics

Jean-François M. Barthelemy
and Fred D. Bergen

NASA

NASA Technical Paper 2808

1988

Shape Sensitivity Analysis of Wing Static Aeroelastic Characteristics

Jean-François M. Barthelemy
Langley Research Center
Hampton, Virginia

Fred D. Bergen
Virginia Polytechnic Institute and State University
Blacksburg, Virginia

National Aeronautics and Space Administration

Scientific and Technical Information Division

Abstract

A method is presented to calculate analytically the sensitivity derivatives of wing static aeroelastic characteristics with respect to wing shape parameters. The wing aerodynamic response under fixed total load is predicted with Weissinger's L-method; its structural response is obtained with Giles' equivalent plate method. The characteristics of interest in this study include the spanwise distribution of lift, trim angle of attack, rolling and pitching moments, induced drag, as well as the divergence dynamic pressure. The shape parameters considered are the wing area, aspect ratio, taper ratio, sweep angle, and tip twist angle. Results of sensitivity studies indicate that (1) approximations based on analytical sensitivity derivatives can be used for wide ranges of variations of the shape parameters considered, and (2) the analytical calculation of sensitivity derivatives is significantly less expensive than the conventional finite-difference alternative.

Introduction

During the design phase of an engineering system, numerous analyses are conducted to predict changes in the characteristics of the system due to changes in design variables. Usually, this process entails perturbing each variable in turn, recalculating the characteristics, and evaluating the sensitivities with some sort of finite-difference process. The repeated analyses can drive the cost of design very high. An approach that has found increased interest recently in engineering design is analytical calculation of the sensitivity derivatives (Adelman and Haftka, 1987). Typically, the analytical approach requires less computational resource than the finite-difference approach and is less subject to numerical errors (round-off or truncation). The analytical approach is best developed in parallel with the baseline analysis capability since it uses a significant portion of the numerical information generated during baseline analysis.

In the design of modern aircraft, airframe flexibility is a concern from strength, control, and performance standpoints. To properly account for the aerodynamic and structural implications of flexibility, reliable aeroelastic sensitivity analysis is needed. Therefore, both structural and aerodynamic sensitivity analysis capabilities are necessary.

Structural sensitivity analysis methodology has been available for well over two decades for both sizing (thickness, cross-section properties) and shape (configuration) variables (Adelman and Haftka, 1986). However, aerodynamic sensitivity analysis has been nonexistent until relatively recently. Some limited aerodynamic sensitivity analysis capability was developed for aircraft in subcritical compressible flow (Hawk and Bristow, 1984), but it only handled perturbations in the direction of the thickness of the wing (thickness, camber, or twist distribution). A new approach has been proposed by Yates (1987) that considers general geometry variations including planform for subsonic, sonic, and supersonic unsteady, nonplanar lifting-surface theory.

Aeroelastic sensitivity analysis methodology has also been available for more than two decades for structural sizing variables. (See Haftka and Yates (1976) for an example application.) This is because changes in sizing variables affect exclusively the structural stiffness and mass distribution of the airframe and not its basic geometry. Therefore structural sensitivity analysis capability is sufficient. However, the lack of development in aerodynamic shape sensitivity analysis explains why there are very few results in aeroelastic shape sensitivity analysis.

In a notable exception, Haftka et al. (1987) designed a sailplane wing under aeroelastic constraints and analyzed the design model with vortex lattice and finite element methods. A finite-difference aeroelastic sensitivity analysis capability is made possible by (1) devising a reduced order model to describe the wing static aeroelastic response and (2) using exact perturbation analysis to approximate changes in the vorticity vector with changes in the geometry. Because it retains techniques from both analytical and finite-difference sensitivity methodologies, this approach to sensitivity analysis should be described as semianalytical.

The present study is a proof-of-concept that demonstrates the feasibility of calculating analytically the sensitivity of wing static aeroelastic characteristics to changes in wing shape. Of interest also is whether the curvature of the aeroelastic characteristics is small enough that analytical sensitivity derivatives can be used to approximate them without costly reanalyses. The flight regime is chosen to be subsonic and subcritical so that simple and inexpensive structural and aerodynamic analysis methodologies can be used. Yet the results are felt realistic enough that they may be used in conceptual design. It must be noted that the conclusions drawn here are strictly applicable to the analysis methodologies used here and may not hold true for other cases.

This paper first describes the aeroelastic analysis methodology used. It combines Weissinger's L-method (Weissinger, 1947) to predict the wing spanwise lift distribution with Giles' equivalent plate analysis method (Giles, 1986) for structural analysis. The calculation of the sensitivity derivatives is described next. Finally, the methodology is used to investigate the sensitivity of a forward-swept wing to changes in wing area, aspect and taper ratios, and sweep and tip twist angles. The results are analyzed from the standpoints of both accuracy and computational cost. While the development of the sensitivity equations is given in the body of the text, the details of the derivation of the coefficients in those equations are given in appendices A–D.

Nomenclature

a_1	chordwise position of the wing-box leading edge, normalized by the chord, measured from the leading edge
a_2	chordwise position of the wing-box trailing edge, normalized by the chord, measured from the leading edge
A	wing aspect ratio
$[A]$	aerodynamic matrix
b	wingspan
c_r	root chord
c_t	tip chord
$\{cc_l\}$	vector of product of section lift coefficients and chord length at aerodynamic control stations
$c_{l\alpha}$	airfoil lift-curve slope
$[C]$	matrix as defined by equation (A10)
CPU	central processing unit
d	wing-box depth
D_i	induced drag
$[D]$	matrix as defined by equation (A12)
e	position of airfoil center of pressure measured from the quarter-chord point, positive upstream, normalized by the chord
$\{e\}$	eigenvector, see equation (12)
$\{e^r_D\}$, $\{e^l_D\}$	right and left eigenvectors at divergence
E	modulus of elasticity
$[E]$	matrix as defined by equation (D2)
$\{f\}$	vector of applied point loads

G	shear modulus
$h(x,y)$	transverse displacement of the wing surface
$[I]$	identity matrix
$[K]$	stiffness matrix
L	lift
LE	leading edge
M	flight Mach number
M_r	rolling moment
n_a	number of aerodynamic boundary-condition control points along semispan
n_l	number of applied point loads along semispan
n_s	number of terms in the approximation to the wing displacement function
N_x	order of x in the polynomial displacement function $h(x,y)$
N_y	order of y in the polynomial displacement function $h(x,y)$
p	generic wing shape parameters
q	dynamic pressure
q_D	divergence dynamic pressure
$\{s\}$	vector of amplitudes in the wing transverse displacement function (eq. (3))
S	wing area
t	wing skin thickness
TE	trailing edge
T_r	pitching moment
$\{u\}$	vector of 1
$[V]$	diagonal matrix of integration weights
$\{w(x,y)\}$	vector of displacement shape functions (eq. (3))
$[W]$	W_{ij} is the value of entry j of vector $\{w\}$ at the point of application of load i
$[W_x]$	W_{xij} is the value of the streamwise derivative of entry j of vector $\{w\}$ at control station i
x	chordwise coordinate, positive downstream
y	spanwise coordinate, positive out right wing
α_o	wing root angle of attack
$\{\alpha\}$	vector of angles of attack at aerodynamic control stations
$\{\varepsilon\}$	vector of rigid twist angles at aerodynamic control stations
ε_t	wingtip twist angle, positive nose-up
η	normalized spanwise coordinate, $\frac{2y}{b}$

$\{\theta\}$	vector of elastic twist angles at aerodynamic control stations
λ	taper ratio
Λ	quarter-chord sweep angle, positive for sweepback
ν	Poisson's ratio

Special Notations:

$\{\ \}$	column vector
$[\ ]$	square matrix
$(\ )^t$	transposed quantity
$[\ ]^{-1}$	inverse matrix
$(\ )'$	$\partial(\ )/\partial p$

Aeroelastic Analysis

Aerodynamic Model

The wing aerodynamic response is predicted by Weissinger's L-method (Weissinger, 1947), which was used herein as implemented for computations by DeYoung and Harper (1948). It is valid for moderate-to-high-aspect-ratio wings that are symmetric with respect to the root chord, have a straight quarter-chord line over each semispan, and have no discontinuities in twist. The airfoil section properties are assumed known and the flight regime may be compressible although it must be subcritical. In this method, the flow around the wing is modeled by a lifting line of vortices bound at the wing quarter-chord line. A no-penetration boundary condition is specified at n_a control stations and that determines the spanwise distribution of vortex strength. Weissinger (1947) applies the boundary conditions at the three-quarter-chord point of each station; DeYoung and Harper (1948) modify that position to account for lift-curve slopes of less than the theoretical 2π and also for effects of compressibility. A linear relationship between the vectors of local angles of attack and lift at the control stations results:

$$\{\alpha\} = \frac{1}{2b}[A]\{cc_l\} \tag{1}$$

The aerodynamic matrix $[A]$ depends on the airfoil properties and the Mach number as well as the wing shape. Further details are given in appendix B. The total lift developed by the full-span wing is then given by:

$$L = \frac{1}{2}bq\{u\}^t[V]\{cc_l\} \tag{2}$$

Diagonal ($n_a \times n_a$) matrix $[V]$ contains shape-independent integration weights; its derivation is detailed in appendix A.

Structural Model

Giles' equivalent plate analysis method assumes that the wing behaves like a plate and that its transverse displacements can be modeled by a polynomial in the chordwise and spanwise coordinates

$$h(x,y) = \{w(x,y)\}^t\{s\} \tag{3}$$

where vector $\{w\}$ contains n_s products of various powers of x and y. A careful selection of the exponents of the variables permits the specification of various types of boundary

conditions at the wing root. By applying the principle of virtual work, the wing static equilibrium equation under a vector $\{f\}$ of n_l point loads is obtained

$$[K]\{s\} = [W]^t\{f\} \tag{4}$$

The stiffness matrix $[K]$ is consistent with the displacements given in equation (3); it is a function of the wing shape and sizing variables as well as wing material properties. This approach has shown very good results for both static and dynamic analysis of wings (Giles, 1986 and 1987). It can handle fairly general planform geometries and boundary conditions, model complex wing cross-section geometries, include rib and spar caps, and permit the use of composite materials and the consideration of thermal loading.

Aeroelastic Response

To proceed with the calculation of the spanwise distribution of lift and the trim angle of attack under fixed lift, the vector of applied point loads is written in terms of the aerodynamic loads (see appendix A):

$$\{f\} = \frac{1}{4}bq[V]\{cc_l\} \tag{5}$$

The vector of angles of attack can be written as follows:

$$\{\alpha\} = \alpha_o\{u\} + \{\varepsilon\} + \{\theta\} \tag{6}$$

All the entries of $\{u\}$ are 1. Vector $\{\theta\}$ can be derived from equation (3). At any control point i, the elastic twist is given by

$$\theta_i = -\frac{\partial}{\partial x}h(x_i, y_i)$$

For consistency with the aerodynamic model, the elastic twist is measured at the three-quarter chord. Then,

$$\{\theta\} = -[W_x]\{s\} \tag{7}$$

Combining equations (1), (4)–(7), as well as trim equation (2), we obtain the unknown angle of attack and the spanwise distribution of lift from:

$$\begin{bmatrix} [A] + \frac{qb^2}{2}[W_x][K]^{-1}[W]^t[V] & -2b\{u\} \\ \frac{b}{2}\{u\}^t[V] & 0 \end{bmatrix} \begin{Bmatrix} \{cc_l\} \\ \alpha_o \end{Bmatrix} = \begin{Bmatrix} 2b\{\varepsilon\} \\ \frac{L}{q} \end{Bmatrix} \tag{8}$$

Note that the inversion of the stiffness matrix precludes the use of free-body modes. Spanwise integration of the distribution of lift yields the rolling and pitching moments

$$M_r = \frac{qb^2}{8}\{u\}^t[V][C]\{cc_l\} \tag{9}$$

$$T_r = \frac{qb}{4}\{u\}^t[V][D]\{cc_l\} \tag{10}$$

The total induced drag is given by DeYoung and Harper (1948) as

$$D_i = \frac{\pi q}{8n_a}\{cc_l\}^t[E]\{cc_l\} \tag{11}$$

Matrices $[C]$ and $[E]$ are independent on the wing shape; their derivation is given in appendices A and D, respectively. Matrix $[D]$ is dependent on the wing shape; its derivation is given in appendix A.

One can obtain rigid-wing aerodynamic results for the analysis by setting q to zero in the left-hand side of equation (8) and performing the calculations of equations 9–11.

Finally, the wing divergence dynamic pressure is found as the lowest eigenvalue q of the fixed-angle-of-attack problem:

$$\left[[A] + q\left[\frac{b^2}{2}[W_x][K]^{-1}[W]^t[V]\right]\right]\{e\} = \{0\} \tag{12}$$

where $\{e\}$ is the eigenvector. The matrices in equation (12) are nonsymmetric; therefore, the system has distinct right and left eigenvectors.

Aeroelastic Sensitivity Analysis

Sensitivity analysis begins with calculation of the derivatives of the distribution of lift and trim angle of attack. Taking the derivative of equation (8) with respect to p, we obtain after rearranging:

$$\begin{bmatrix} [A] + \frac{qb^2}{2}[W_x][K]^{-1}[W]^t[V] & -2b\{u\} \\ \frac{b}{2}\{u\}^t[V] & 0 \end{bmatrix} \begin{Bmatrix} \{cc_l\} \\ \alpha_o \end{Bmatrix}'$$

$$= \left\{ \begin{Bmatrix} 2(b'\{\varepsilon\} + b\{\varepsilon\}') \\ 0 \end{Bmatrix} - \begin{bmatrix} [A]' + \frac{q}{2}\left[b^2[W_x][K]^{-1}[W]^t\right]'[V] & -2b'\{u\} \\ \frac{b'}{2}\{u\}^t[V] & 0 \end{bmatrix} \begin{Bmatrix} \{cc_l\} \\ \alpha_o \end{Bmatrix} \right\} \tag{13}$$

As for all sensitivity equations, this equation is linear. The coefficient matrix on the left-hand side is identical to that of equation (8), which gives the distribution of lift and angle of attack. Further, it does not depend on the parameter with respect to which sensitivity is sought (a similar formulation is used by Yates (1987)). Therefore, only one calculation and inversion or factorization of the matrix is necessary for analysis and complete sensitivity analysis. There is one right-hand-side vector for each parameter of interest. The derivative of the matrix product $[b^2[W_x][K]^{-1}[W]^t]$ is found by expansion. Calculations for the derivatives of the semispan b and the vector of twist $\{\varepsilon\}$, the aerodynamic matrix $[A]$, and the matrices $[W_x]$ and $[W]$ are found in appendices A, B, and C, respectively. The derivatives of the flexibility matrix ($[K]^{-1}$) are obtained from those of the stiffness matrix. Indeed,

$$[K][K]^{-1} = [I]$$

After taking the derivatives and rearranging,

$$[K]^{-1\prime} = -[K]^{-1}[K]'[K]^{-1} \tag{14}$$

In the present application, even though the sensitivity analysis is performed analytically, the derivatives of the stiffness matrix are found by finite difference. This practice makes the implementation almost as simple as for finite-difference sensitivity analysis while preserving much of the accuracy and cost advantages of the analytical approach.

The shape derivatives of the rolling and pitching moments as well as the induced drag are obtained from equations (9)–(11). We have

$$M_r' = \frac{q}{8}\{u\}^t[V]\{2bb'[C]\{cc_l\} + b^2[C]\{cc_l\}'\} \tag{15}$$

$$T_r' = \frac{q}{4}\{u\}^t[V]\{b'[D]\{cc_l\} + b[D]'\{cc_l\} + b[D]\{cc_l\}'\} \tag{16}$$

$$D_i' = \frac{\pi q}{8n_a}(\{cc_l\}'^t[E]\{cc_l\} + \{cc_l\}^t[E]\{cc_l\}') \tag{17}$$

The details of the calculations for matrix $[D]'$ are found in appendix A. Rigid-wing results can be obtained if the dynamic pressure is set to zero in equation (13).

The derivatives of the divergence dynamic pressure are found from equation (12). If q_D is the divergence dynamic pressure and $\{e_D^r\}$ is the right eigenvector, we have

$$\left[[A] + q_D\left[\frac{b^2}{q}[W_x][K]^{-1}[W]^t[V]\right]\right]\{e_D^r\} = \{0\} \tag{18}$$

Taking the derivative of this expression, premultiplying by the transposed left eigenvector $\left\{e_D^l\right\}^t$, and rearranging, we find

$$q_D' = \frac{\{e_D^l\}^t\left[[A]' + \frac{q_D}{2}\left[b^2[W_x][K]^{-1}[W]^t\right]'[V]\right]\left\{e_D^r\right\}}{\left\{e_D^l\right\}^t\left[\frac{b^2}{2}q_D[W_x][K]^{-1}[W]^t[V]\right]\left\{e_D^r\right\}} \tag{19}$$

Most of the matrix manipulations required in equation (19) were already performed while the derivatives of lift distribution and angle of attack were calculated. Therefore all that is necessary to evaluate the divergence dynamic pressure derivative is the calculation of the left-hand eigenvector.

Applications

The procedure described here was implemented on a MicroVAX II workstation in FORTRAN. Qualitatively, as can be inferred from the derivations, the development and implementation of the sensitivity analysis procedure are little more involved than those of the analysis procedure itself. This section of the paper describes some numerical applications.

The wing model is described by five independent shape parameters: wing area S, aspect ratio A, taper ratio λ, quarter-chord sweep angle Λ, and tip twist angle ε_t. The model geometry is depicted in figure 1, and the problem parameters are given in table I.

The number n_a of aerodynamic control stations was varied to examine convergence and 30 was felt adequate; the effect of varying n_a on accuracy and computational cost will be taken up in a subsequent section of this report.

The wing structure is an aluminum wing-box of constant depth d and made of two flat cover skins of constant thickness t; it is located between the constant chord locations a_1 and a_2.

A measure of the flexibility of this wing is its divergence dynamic pressure of 16.3 kPa. For an air density of 1 kg/m^3, the airspeed at which the elastic calculations are performed is 89.4 m/sec, and the divergence speed is about twice as much at 180.3 m/sec.

Results

Sensitivity Results

A sensitivity analysis is performed for the baseline design, and derivatives are generated analytically for rigid-wing and elastic-wing characteristics with respect to the five independent shape parameters. The characteristics include the rigid and elastic spanwise lift distribution (only wingtip values are given here, since they exhibit maximum aeroelastic effects), trim angle of attack, rolling and pitching moments, induced drag, and divergence dynamic pressure. These derivatives are used to approximate changes in the characteristics due to changes in the shape parameters. If $r(p)$ is the value of characteristic r for a value p of a shape parameter, and if $r'(p)$ is the sensitivity derivative of r at p with respect to p, then, for a small Δp, we can write:

$$r(p + \Delta p) \cong r(p) + r'(p)\Delta p \tag{20}$$

In order to gauge the quality of the approximations, exact values of the perturbed characteristic $r(p + \Delta p)$ are generated by reanalysis for each value of Δp. Figures 2–7 give examples of the sensitivity results so generated. All the figures share the same layout with the varied independent parameter on the horizontal axis and the characteristic on the vertical axis. Sensitivity results are given for both rigid- and elastic-wing cases.

The results display two important properties. First, the straight lines of equation (20) are tangent to the corresponding sensitivity curves at the baseline values of the shape parameters, as, of course, they should be. Second, the curvatures of the characteristics are small enough so that sensitivity-derivative-based extrapolations can be used to approximate them for a wide range of variation of the shape parameters considered. The range of parameter variations for which the approximations are accurate enough depends largely on the application considered and the stage in the design process. Usually, however, the variations considered in a design effort are significantly smaller than those used in the present calculations, and the quality of the linear approximations should be quite adequate. Indeed, for parameter variations of ±10 percent (±1° for the twist angle), the relative prediction error (|(actual value − predicted value)/actual value |) never exceeds 1 percent in the results given here. Such a conclusion might differ in flight conditions that involve more complex flows as in the presence of shock waves or strong viscous interactions.

Convergence of Calculated Parameters With Respect to n_a

The discretization of the aerodynamic model (n_a) is varied to assess its effect on convergence of the parameters and their derivatives. While n_a is varied, the discretization of the structural model is held fixed ($N_x = 5$, $N_y = 6$) because, as indicated by Giles (1986), it cannot be increased significantly without risking singularities in the stiffness matrix.

Table II shows the effect that aerodynamic discretization has on the convergence of the induced drag, the divergence dynamic pressure, as well as their derivatives. The induced drag and its derivatives converge more slowly than the divergence dynamic pressure. This is probably because the induced drag is very sensitive to variations in the shape of the load distribution and that the latter is slow to converge itself. For all the other characteristics considered, the trend is similar to that displayed by the divergence dynamic pressure. Note that, in both cases, the sensitivity derivatives of the characteristics converge about as fast as the characteristics themselves.

Computational Cost

Figures 8 and 9 show the effect that aerodynamic model discretization has on computational cost and its major components for generation of the sensitivity derivatives by finite difference and analytically. The cost is estimated in terms of both CPU time and total number of floating-point operations. The latter number is based on a double-precision LINPAK computing speed of .16 MFLOPS for a MicroVAX II workstation (Dongarra, 1985). For finite-difference sensitivity analysis, the cost only includes that of five full reanalyses (one for each independent shape parameter); no effort was made to avoid repeated calculations of invariant quantities. The cost of analytical calculation of the sensitivity derivatives is significantly lower than that of the finite-difference approach; the difference increases as the discretization is refined. For more elaborate analytical procedures that involve two-dimensional (surface panel) or three-dimensional (volume grid) discretizations, this effect is expected to become more pronounced.

For both approaches, the cost associated with the calculations of the stiffness matrix and its derivatives remains constant since the structural model is unchanged. For the finite difference approach, the calculation of the aerodynamic matrix and its derivatives by finite difference is by far the major contributor to the total cost. For the analytical approach two items dominate the total cost for the finer discretization. First comes the cost of calculating the matrices $[W]$ and $[W_x]$, their derivatives, and the multiplications associated with changes between the discretization of the aerodynamic model and that of the structural model. Second

is that of the input/output operations relating to the transfer of information generated during analysis to the sensitivity analysis code. In fact the cost of computing the derivatives of the aerodynamic matrix is so small that it is not shown on the graph.

Although the cost breakdowns discussed here may not be representative of those obtained with other analysis codes or other computer implementations, these results point to a cost advantage for the analytical approach to sensitivity analysis.

Conclusions

The results presented in this study show that, for subsonic subcritical flow, the curvatures of the wing aeroelastic characteristics are small enough that the characteristics can be well approximated by sensitivity-derivative-based linear extrapolations over ranges of variation of the shape parameters that are wide enough to be useful during the design process. Also, the analytical computation of the sensitivity derivatives is significantly less expensive computationally than the conventional finite-difference approach. In addition, with the simple aerodynamic and structural models used here, the derivation and implementation of the sensitivity analysis capability are little more complex than those of the corresponding analysis capability.

NASA Langley Research Center
Hampton, VA 23665-5225
March 29, 1988

Appendix A

Aerodynamically Related Geometrical Parameters and Derivatives

As shown in figure 10, the wing has a trapezoidal planform. The wing shape is completely described by five independent shape parameters: wing area S, aspect ratio A, taper ratio λ, quarter-chord sweep angle Λ, and tip twist angle ε_t. The wing span b and the root and tip chords are dependent variables. They are found as

$$b = \sqrt{AS} \tag{A1}$$

$$c_r = \frac{2}{1+\lambda}\sqrt{\frac{S}{A}} \tag{A2}$$

$$c_t = \frac{2\lambda}{1+\lambda}\sqrt{\frac{S}{A}} \tag{A3}$$

The wing twist varies linearly between 0 at the wing root and ε_t at the wingtip. At a given spanwise location $\eta = 2y/b$, the twist angle is

$$\varepsilon(\eta) = \eta\varepsilon_t \tag{A4}$$

Also, the wing chord $c(\eta)$ is given by

$$c(\eta) = \frac{2\Big(1 + (\lambda - 1)\eta\Big)}{1+\lambda}\sqrt{\frac{S}{A}} \tag{A5}$$

There are n_a control stations in the aerodynamic model. They are defined so that their density increases toward the wingtip. The spanwise position of station i is

$$\eta_i = \frac{2y_i}{b} = \cos\phi_i = \cos\frac{i\pi}{2n_a} \tag{A6}$$

Given the distribution $\{\alpha\}$ of angle of attack at those stations, the aerodynamic analysis determines the corresponding distribution of lift $\{cc_l\}$. (See eq. (1).) For the sake of transferring the loads to the structural model, the distribution is replaced by a vector of point loads as illustrated in figure 11. At station i, the lifting load is given by

$$f_i = \frac{b}{4}qcc_{li}(\eta_{i-1} - \eta_{i+1}) \tag{A7}$$

with

$$f_1 = \frac{b}{4}qcc_{l1}(1 - \eta_2)$$

$$f_{n_a} = \frac{b}{4}qcc_{ln_a}(\eta_{n_a} - 1)$$

In vector form, we have

$$\{f\} = \frac{1}{4}bq[V]\{cc_l\} \tag{A8}$$

with

$$[V] = \text{diag}\,[1 - \eta_2, \eta_1 - \eta_3, ..., \eta_{i-1} - \eta_{i+1}, ..., \eta_{n_a} - 1]$$

where $[V]$ is a shape independent matrix. The total lift on both wings is obtained by summing up the point loads:

$$L = \frac{1}{2} bq \{u\}^t [V] \{cc_l\} \tag{A9}$$

where all the entries of $\{u\}$ are 1. This equation is equivalent to the trapezoid integration rule. The moment of point load f_i with respect to the wing root is given by:

$$m_i = \frac{b}{2} \eta_i f_i$$

so that the rolling moment is given by

$$M_r = \frac{qb^2}{8} \{u\}^t [V][C] \{cc_l\} \tag{A10}$$

with

$$[C] = \text{diag}\,[\eta_1, \eta_2, ..., \eta_i, ..., \eta_{n_a}]$$

and matrix $[C]$ is shape independent. Finally, as shown in figure 10, the pitching moment of f_i with respect to the y-axis is (positive leading-edge up)

$$t_i = -x_{wi} f_i \tag{A11}$$

with

$$x_{wi} = \frac{c_r}{4} + \eta_i \frac{b}{2} \tan \Lambda - ec(\eta_i)$$

where e, an airfoil property input into the calculations, is the distance between the center of pressure and the quarter-chord point normalized by the chord length; it is positive if the center of pressure is ahead of the quarter-chord point. The total pitching moment is then given by

$$T_r = \frac{qb}{4} \{u\}^t [V][D] \{cc_l\} \tag{A12}$$

where

$$[D] = \text{diag}\,[-x_{w1}, -x_{w2}, ..., -x_{wi}, ..., -x_{wn_a}]$$

The derivatives b', $\{\varepsilon\}'$, and $[D]'$, with respect to the independent variables S, A, Λ, λ, and ε_t can be now traced through the expressions given in this appendix.

Appendix B

Aerodynamic Matrix and Derivatives

The derivation of $[A]$ is detailed by DeYoung and Harper (1948). If the unknown distribution of circulation on the wing is approximated by n_a terms of a Fourier series, specification of the no-penetration boundary conditions at n_a control points (eq. (A6)) yields equation (1). $[A]$ can be rewritten:

$$[A] = [B] - \frac{1}{4n_a}[H][L][F] \tag{B1}$$

The expressions in this appendix are given for symmetric loading; they include compressibility corrections and allow for input of section lift curve slope. Matrices $[B]$ and $[F]$ are shape independent; they are given in terms of the angles ϕ_i (eq. (A6)) by

$$\left.\begin{aligned}
B_{ij} &= -2(b_{ij} + b_{i2n_a-j}) && \text{if } i \neq j,\ j \neq n_a \\
&= -2b_{in_a} && i \neq j,\ j = n_a \\
&= 2b_{ii} && i = j,\ j \neq n_a \\
&= 2b_{n_a n_a} && i = j,\ j = n_a \\
b_{ij} &= \frac{\sin\phi_j}{(\cos\phi_j - \cos\phi_i)^2}\left(\frac{1-(-1)^{j-i}}{4n_a}\right) && i \neq j \\
b_{ii} &= \frac{n_a}{2\sin\phi_i}
\end{aligned}\right\} \tag{B2}$$

and

$$\left.\begin{aligned}
F_{ij} &= \frac{2}{n_a} f_{ij} && \text{if } i \neq 1,\ j \neq n_a \\
&= \frac{1}{n_a} f_{ij} && i = 1,\ j \neq n_a \\
&= \frac{1}{n_a} f_{ij} && i \neq 1,\ j = n_a \\
&= \frac{1}{2n_a} f_{ij} && i = 1,\ j = n_a \\
f_{ij} &= \sum_{i_1 \text{odd}}^{2n_a-1} i_1 \sin(i_1\phi_j)\cos(i_1\phi_{i-1})
\end{aligned}\right\} \tag{B3}$$

Matrices $[H]$ and $[L]$ depend on the shape parameters exclusively through the following terms:

$$\rho_i = \left(\frac{b}{c_i}\right)_\beta = \frac{2\pi}{c_{l_\alpha}}\left(\frac{b}{c(\eta_i)}\right) \tag{B4}$$

$$\tau = \tan\Lambda_\beta = \frac{\tan\lambda}{\sqrt{1-M^2}} \tag{B5}$$

where c_{l_α} and M are respectively the airfoil lift curve slope and the flight Mach number. Matrix $[H]$ is

$$[H] = \text{diag}\,[\rho_1, \rho_2, ..., \rho_i, ..., \rho_{n_a}] \tag{B6}$$

Matrix $[L]$ is given by

$$L_{ij} = \frac{N1_{ij} - 1}{D1_{ij}} + \frac{1}{D21_{ij}}\left(\frac{N2_{ij}}{D22_i} - 1\right) + \frac{N31\ N32_i}{D22_i} \tag{B7}$$

and

$$N1_{ij} = \sqrt{\left(1 + \rho_i(\eta_i - \eta_j)\tau\right)^2 + \rho_i^2(\eta_i - \eta_j)^2} \qquad D1_{ij} = \rho_i(\eta_i - \eta_j)$$

$$N2_{ij} = \sqrt{\left(1 + \rho_i(\eta_i - \eta_j)\tau\right)^2 + \rho_i^2(\eta_i + \eta_j)^2} \qquad D21_{ij} = \rho_i(\eta_i + \eta_j)$$

$$D22_i = 1 + 2\rho_i\eta_i\tau$$

$$N31 = 2\tau \qquad N32_i = \sqrt{(1 + \rho_i\eta_i\tau)^2 + \rho_i^2\eta_i^2}$$

Because only matrices $[H]'$ and $[L]$ depend on the wing shape, the derivative of $[A]$ with respect to any shape parameter p reads

$$[A]' = -\frac{1}{4n_a}[[H]'[L] + [H][L]'][F] \tag{B8}$$

The derivatives $[H]'$, can be determined from equations (A1), (A5), (B4), and (B6). For $[L]'$, we have, for any shape parameter p

$$\frac{\partial L_{ij}}{\partial p} = \frac{\partial L_{ij}}{\partial \rho_i}\frac{\partial \rho_i}{\partial p} + \frac{\partial L_{ij}}{\partial \tau}\frac{\partial \tau}{\partial p} \tag{B9}$$

Derivatives $\partial\rho_i/\partial p$ and $\partial\tau/\partial p$ can be determined from equations (A1), (A5), (B4), and (B5). Now, if σ stands for either ρ_i or τ, we have

$$\frac{\partial L_{ij}}{\partial \sigma} = \frac{1}{D1_{ij}}\frac{\partial N1_{ij}}{\partial \sigma} - \frac{(N1_{ij} - 1)}{D1_{ij}^2}\frac{\partial D1_{ij}}{\partial \sigma} - \frac{1}{D21_{ij}^2}\left(\frac{N2_{ij}}{D22_i} - 1\right)\frac{\partial D21_{ij}}{\partial \sigma}$$

$$+ \frac{1}{D21_{ij}}\left(\frac{1}{D22_i}\frac{\partial N2_{ij}}{\partial \sigma} - \frac{N2_{ij}}{D22_i^2}\frac{\partial D22_i}{\partial \sigma}\right) + \frac{N32_i}{D22_{ij}}\frac{\partial N31}{\partial \sigma}$$

$$+ \frac{N31}{D22_i}\frac{\partial N32_i}{\partial \sigma} - \frac{N31 N32_i}{D22_i^2}\frac{\partial D22_i}{\partial \sigma} \tag{B10}$$

and

$$\frac{\partial N1_{ij}}{\partial \rho_i} = \frac{1}{N1_{ij}}\left((1+\rho_i(\eta_i-\eta_j)\tau)(\eta_i-\eta_j)\tau + \rho_i(\eta_i-\eta_j)^2\right)$$

$$\frac{\partial N1_{ij}}{\partial \tau} = \frac{1}{N1_{ij}}\left(1+\rho_i(\eta_i-\eta_j)\tau\right)\rho_i(\eta_i-\eta_j)$$

$$\frac{\partial D1_{ij}}{\partial \rho_i} = (\eta_i-\eta_j) \qquad \frac{\partial D1_{ij}}{\partial \tau} = 0$$

$$\frac{\partial N2_{ij}}{\partial \rho_i} = \frac{1}{N2_{ij}}\left((1+\rho_i(\eta_i-\eta_j)\tau)(\eta_i-\eta_j)\tau + \rho_i(\eta_i+\eta_j)^2\right)$$

$$\frac{\partial N2_{ij}}{\partial \tau} = \frac{1}{N2_{ij}}\left(1+\rho_i(\eta_i-\eta_j)\tau\right)\rho_i(\eta_i-\eta_j)$$

$$\frac{\partial D21_{ij}}{\partial \rho_i} = (\eta_i+\eta_j) \qquad \frac{\partial D21_{ij}}{\partial \tau} = 0$$

$$\frac{\partial D22_i}{\partial \rho_i} = 2\eta_i\tau \qquad \frac{\partial D22_i}{\partial \tau} = 2\rho_i\eta_i$$

$$\frac{\partial N31_i}{\partial \rho_i} = 0 \qquad \frac{\partial N31_i}{\partial \tau} = 2$$

$$\frac{\partial N32_i}{\partial \rho_i} = \frac{1}{N32_i}\left((1+\rho_i\eta_i\tau)\eta_i\tau + \rho_i\eta_i^2\right) \qquad \frac{\partial N32_i}{\partial \tau} = \frac{1}{N32_i}(1+\rho_i\eta_i\tau)\rho_i\eta_i$$

When evaluating terms on the diagonal of $\partial L/\partial \rho_i$, care must be taken because the first term of equation (B10) becomes indefinite for $i = j$. Using L'Hospital's rule, it can be shown that

$$\text{if } \eta_i \to \eta_j, \text{ then } \frac{1}{D1_{ij}}\frac{\partial N1_{ij}}{\partial \rho_i} - \frac{(N1_{ij}-1)}{D1_{ij}^2}\frac{\partial D1_{ij}}{\partial \rho_i} \to 0$$

Appendix C

$[W]$ and $[W_x]$ Matrices and Derivatives

The term W_{ij} was defined previously as the value of the jth approximation function at the point of application of the ith load in the assumed displacement function of the equivalent plate analysis method. The jth approximation function reads as follows:

$$w_j = \left(\frac{x}{x_{\max}}\right)^{n_{xj}} \left(\frac{y}{y_{\max}}\right)^{n_{yj}} \tag{C1}$$

For wings clamped at the root, n_{xj} takes all the values between 0 and N_x; for a given n_{xj}, n_{yj} varies between 2 and N_y. The N_x and N_y values are chosen by the user; Giles (1986) suggests an upper limit of 7 for both of them. Also defined by the user are constant normalization lengths $x_{\max}$ and $y_{\max}$. As detailed in appendix A, the aerodynamic loading is replaced by an equivalent set of point loads at the n_a aerodynamic control stations. Therefore, we have for point i (see fig. 10)

$$\left.\begin{aligned} x_{wi} &= \frac{c_r}{4} + \eta_i \frac{b}{2}\tan\Lambda - ec(\eta_i) \\ y_{wi} &= \frac{b}{2}\eta_i \end{aligned}\right\} \tag{C2}$$

The parameters b, c_r, $c(\eta)$, and η_i are defined in terms of the wing independent shape variables in equations (A1), (A2), (A5), and (A6), respectively. If p is any of the independent shape parameters (S, A, Λ, and λ) on which the structural model depends, then

$$\frac{\partial W_{ij}}{\partial p} = \frac{\partial w_j}{\partial x_{wi}}\frac{\partial x_{wi}}{\partial p} + \frac{\partial w_j}{\partial y_{wi}}\frac{\partial y_{wi}}{\partial p} \tag{C3}$$

where $\partial w_j/\partial x_{wi}$ and $\partial w_j/\partial y_{wi}$ are calculated from equation (C1). As to $\partial x_{wi}/\partial p$ and $\partial y_{wi}/\partial p$, they are found by combining equations (C2), (A1), (A2), (A5), and (A6). This yields

$$\left.\begin{aligned} \frac{\partial x_{wi}}{\partial S} &= \frac{1-4e(1-\eta_i)+(1+\lambda)\eta_i A\tan\Lambda - 4e\eta_i\lambda}{4\sqrt{AS}(1+\lambda)} & \frac{\partial y_{wi}}{\partial S} &= \frac{\eta_i\sqrt{A}}{4\sqrt{S}} \\ \frac{\partial x_{wi}}{\partial A} &= \frac{\sqrt{S}(-1+4e(1-\eta_i)+4e\eta_i\lambda)}{4\sqrt{A}^3(1+\lambda)} + \frac{\eta_i\sqrt{S}\tan\Lambda}{4\sqrt{A}} & \frac{\partial y_{wi}}{\partial A} &= \frac{\eta_i\sqrt{S}}{4\sqrt{A}} \\ \frac{\partial x_{wi}}{\partial \Lambda} &= \frac{\eta_i b}{2\cos^2\Lambda} & \frac{\partial y_{wi}}{\partial \Lambda} &= 0 \\ \frac{\partial x_{wi}}{\partial \lambda} &= \frac{\sqrt{S}(-2+8e(1-\eta_i)-8\eta_i)}{4\sqrt{A}(1+\lambda)^2} & \frac{\partial y_{wi}}{\partial \lambda} &= 0 \end{aligned}\right\} \tag{C4}$$

The term W_{xij} was defined as the streamwise derivative of the jth approximation function at control station i, in the assumed displacement function of the equivalent plate analysis method. The streamwise derivative of the jth approximation function reads as follows:

$$w_{jx} = \frac{\partial w_j}{\partial x} = \frac{n_{xj}}{x_{\max}}\left(\frac{x}{x_{\max}}\right)^{n_{xj}-1}\left(\frac{y}{y_{\max}}\right)^{n_{yj}} \tag{C5}$$

As mentioned in the discussion pertaining to equation (7), the elastic twist angle is measured at the three-quarter chord position of the aerodynamic model control stations. Therefore, we have for point i (see fig. 10)

$$\left.\begin{aligned} x_{wxi} &= \frac{c_r}{4} + \eta_i \frac{b}{2} \tan\Lambda + \frac{1}{2} c(\eta_i) \\ y_{wxi} &= y_{wi} = \frac{b}{2} \eta_i \end{aligned}\right\} \tag{C6}$$

The parameters b, c_r, $c(\eta)$, and η_i are defined in terms of the wing independent shape variables in equations (A1), (A2), (A5), and (A6), respectively. If p is any of the independent shape parameters (S, A, Λ, and λ) on which the structural model depends, then

$$\frac{\partial W_{xij}}{\partial p} = \frac{\partial}{\partial p} \frac{\partial w_j}{\partial x_{wxi}} = \frac{\partial^2 w_j}{\partial x_{wxi}^2} \frac{\partial x_{wxi}}{\partial p} + \frac{\partial^2 w_j}{\partial x_{xwi} \partial y_{xwi}} \frac{\partial y_{wxi}}{\partial p} \tag{C7}$$

$\partial^2 w_j / \partial x_{wxi}^2$ and $\partial^2 w_j / \partial x_{wxi} \partial y_{wxi}$ are calculated from equation (C5). As to $\partial x_{wxi}/\partial p$ and $\partial y_{wxi}/\partial p$, they are found by combining equations (C6), (A1), (A2), (A5), and (A6). This yields

$$\left.\begin{aligned} \frac{\partial x_{wxi}}{\partial S} &= \frac{3 - 2\eta_i + 2\eta_i\lambda + (1+\lambda)\eta_i A \tan\Lambda}{4\sqrt{AS}(1+\lambda)} & \frac{\partial y_{wxi}}{\partial S} &= \frac{\eta_i \sqrt{A}}{4\sqrt{S}} \\ \frac{\partial x_{wxi}}{\partial A} &= \frac{\sqrt{S}(-3 - 2(1-\lambda)\eta_i)}{4\sqrt{A^3}(1+\lambda)} + \frac{\eta_i \sqrt{S} \tan\Lambda}{4\sqrt{A}} & \frac{\partial y_{wxi}}{\partial R} &= \frac{\eta_i \sqrt{S}}{4\sqrt{A}} \\ \frac{\partial x_{wxi}}{\partial \Lambda} &= \frac{\eta_i b}{2\cos^2\Lambda} & \frac{\partial y_{wxi}}{\partial \Lambda} &= 0 \\ \frac{\partial x_{wxi}}{\partial \lambda} &= \frac{\sqrt{S}(-6 + 8\eta_i)}{4\sqrt{A}(1+\lambda)^2} & \frac{\partial y_{wxi}}{\partial \lambda} &= 0 \end{aligned}\right\} \tag{C8}$$

Appendix D
Drag Matrix

DeYoung and Harper (1948) detail the calculations for the induced drag. In matrix form, the drag is given by

$$D_i = \frac{\pi q}{8n_a}\{cc_l\}^t[E]\{cc_l\} \tag{D1}$$

Matrix $[E]$ is independent of the wing shape; it is given in terms of the angles ϕ_i of equation (A6) and the coefficients b_{ij} of equation (B2):

$$\left.\begin{aligned}
E_{ij} &= -2(b_{ij} + b_{i2n_a-j})\sin\phi_i && \text{if } i \neq j,\ i \neq n_a,\ j \neq n_a \\
&= -2b_{ij}\sin\phi_i && \text{if } i \neq j,\ i \neq n_a,\ j = n_a \\
&= -(b_{ij} + b_{i2n_a-j})\sin\phi_i && \text{if } i \neq j,\ i = n_a \\
&= 2b_{ii}\sin\phi_i && \text{if } i = j,\ i \neq n_a \\
&= b_{n_an_a}\sin\phi_{n_a} && \text{if } i = j,\ i = n_a
\end{aligned}\right\} \tag{D2}$$

References

Adelman, Howard M.; and Haftka, Raphael T. 1986: Sensitivity Analysis of Discrete Structural Systems. *AIAA J.*, vol. 24, no. 5, May, pp. 823–832.

Adelman, Howard M.; and Haftka, Raphael T., compilers 1987: *Sensitivity Analysis in Engineering.* NASA CP-2457.

DeYoung, John; and Harper, Charles W. 1948: *Theoretical Symmetric Span Loading at Subsonic Speeds for Wings Having Arbitrary Plan Form.* NACA Rep. 921.

Dongarra, Jack J. 1985: *Performance of Various Computers Using Standard Linear Equations Software in a FORTRAN Environment.* ANL/MCS-TM-23, Argonne Natl. Lab., July 15.

Giles, Gary L. 1986: Equivalent Plate Analysis of Aircraft Wing Box Structures With General Planform Geometry. *J. Aircr.*, vol. 23, no. 11, Nov., pp. 859–864.

Giles, Gary L. 1987: *Further Generalization of an Equivalent Plate Representation for Aircraft Structural Analysis.* NASA TM-89105.

Haftka, R. T.; Grossman, B.; Eppard, W. M.; and Kao, P. J. 1987: Efficient Optimization of Integrated Aerodynamic-Structural Design. VPI paper presented at the International Conference on Inverse Design Concepts and Optimization in Engineering Sciences—II, ICIDES—II (Pennsylvania State Univ., University Park, Pennsylvania), Oct. 26.

Haftka, Raphael T.; and Yates, E. Carson, Jr. 1976: Repetitive Flutter Calculations in Structural Design. *J. Aircr.*, vol. 13, no. 7, July, pp. 454–461.

Hawk, J. Dennis; and Bristow, Dean R. 1984: *Development of MCAERO Wing Design Panel Method With Interactive Graphics Module.* NASA CR-3775.

Weissinger, J. 1947: *The Lift Distribution of Swept-Back Wings.* NACA TM-1120.

Yates, E. Carson, Jr. 1987: *Aerodynamic Sensitivities From Subsonic, Sonic, and Supersonic Unsteady, Nonplanar Lifting Surface Theory.* NASA TM-100502.

Table I. Baseline Model Parameters

Wing geometry:
- $S = 20\ \text{m}^2$
- $A = 7.5$
- $\lambda = 0.5$
- $\Lambda = -20°$
- $\varepsilon_t = 0°$

Wing structural model:
- $a_1 = 0.2$
- $a_2 = 0.7$
- $t = 0.02$ m
- $d = 0.1$ m

Airfoil properties:
- $c_{l_\alpha} = 6$
- $e = 0$

Structural properties:
- $E = 6.89\ 10^7$ kPa
- $\nu = 0.3$
- $G = 2.65\ 10^7$ kPa

Loading condition:
- $q = 4$ kPa
- $M = 0.5$
- $L = 40\,000$ N

Analytical model discretizations:
- $n_a = n_l = n_s$
- $N_x = 5$
- $N_y = 6$

Table II. Effect of Aerodynamic Model Discretization on Convergence of Elastic Induced Drag and Divergence Dynamic Pressure and Their Derivatives

Characteristics and derivatives	$n_a = 10$	$n_a = 30$	$n_a = 50$	$n_a = 70$
D_i^e, N	859.17	852.70	852.19	852.05
$\partial D_i^e/\partial S$, N/m^2	−42.739	−42.300	−42.266	−42.257
$\partial D_i^e/\partial A$, N	−112.72	−111.64	−111.56	−111.53
$\partial D_i^e/\partial \lambda$, N	24.489	27.686	27.936	28.005
$\partial D_i^e/\partial \Lambda$, N/deg	−0.10177	−0.084786	−0.084135	−0.083973
$\partial D_i^e/\partial \varepsilon$, N/deg	2.3223	2.8464	2.8850	2.8955
q_D, kPa	16.308	16.254	16.250	16.249
$\partial q_D/\partial S$, kPa/m^2	−1.2220	−1.2179	−1.2176	−1.2175
$\partial q_D/\partial A$, kPa	−3.8220	−3.8096	−3.8086	−3.8083
$\partial q_D/\partial \lambda$, kPa	−8.1577	−8.1288	−8.1265	−8.1259
$\partial q_D/\partial \Lambda$, kPa/m^2	6.7952	6.7707	6.7690	6.7685

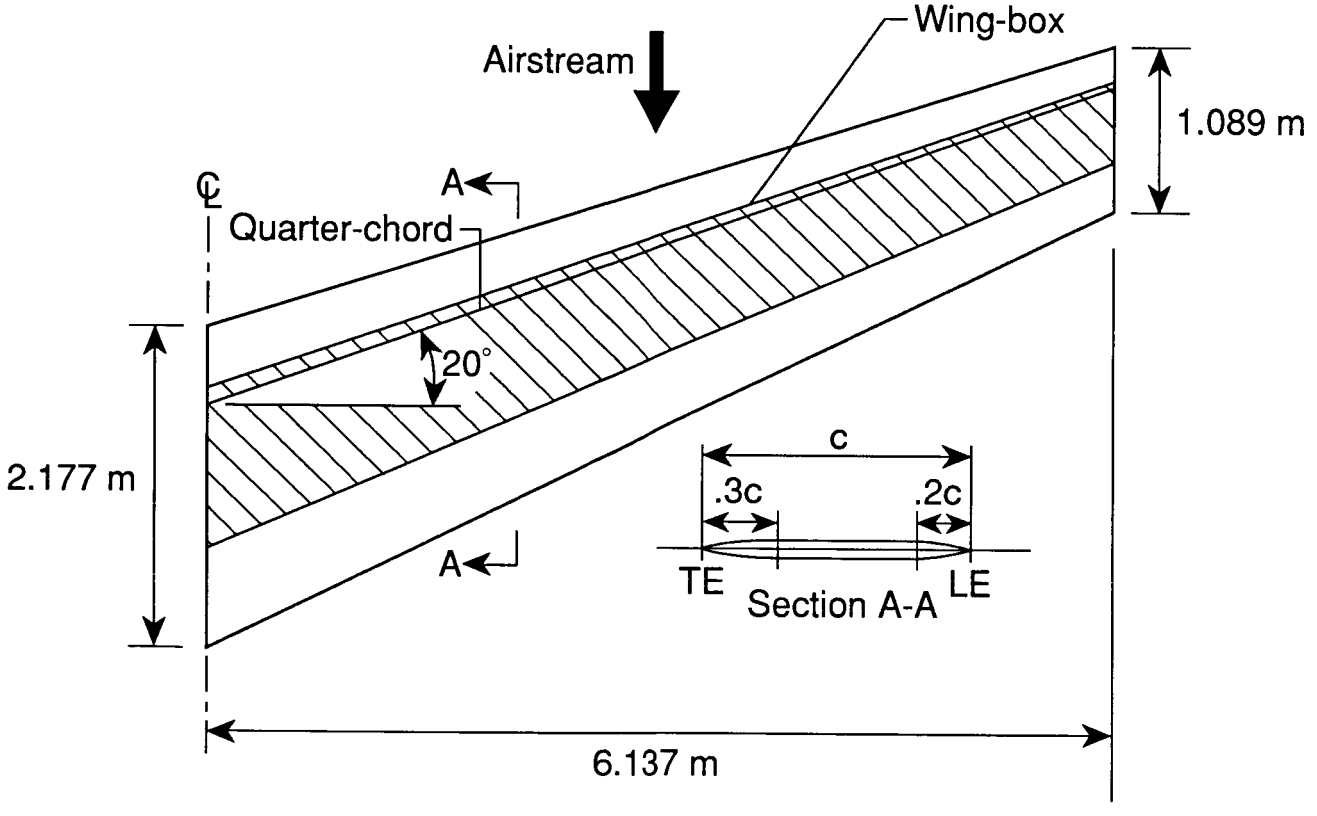

Figure 1. Baseline wing geometry.

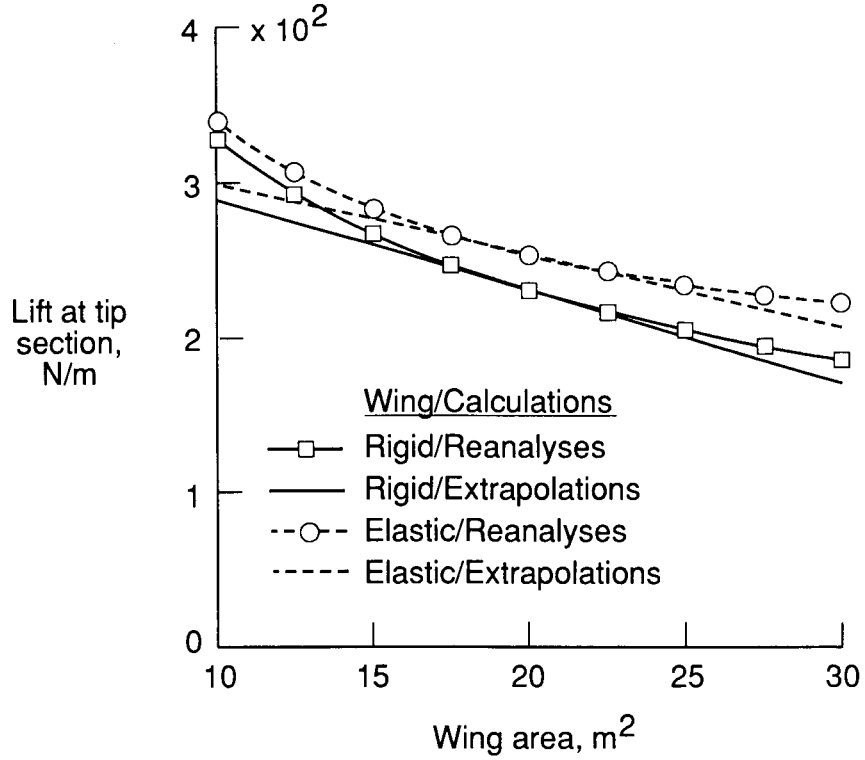

Figure 2. Sensitivity of lift at wingtip station to wing area.

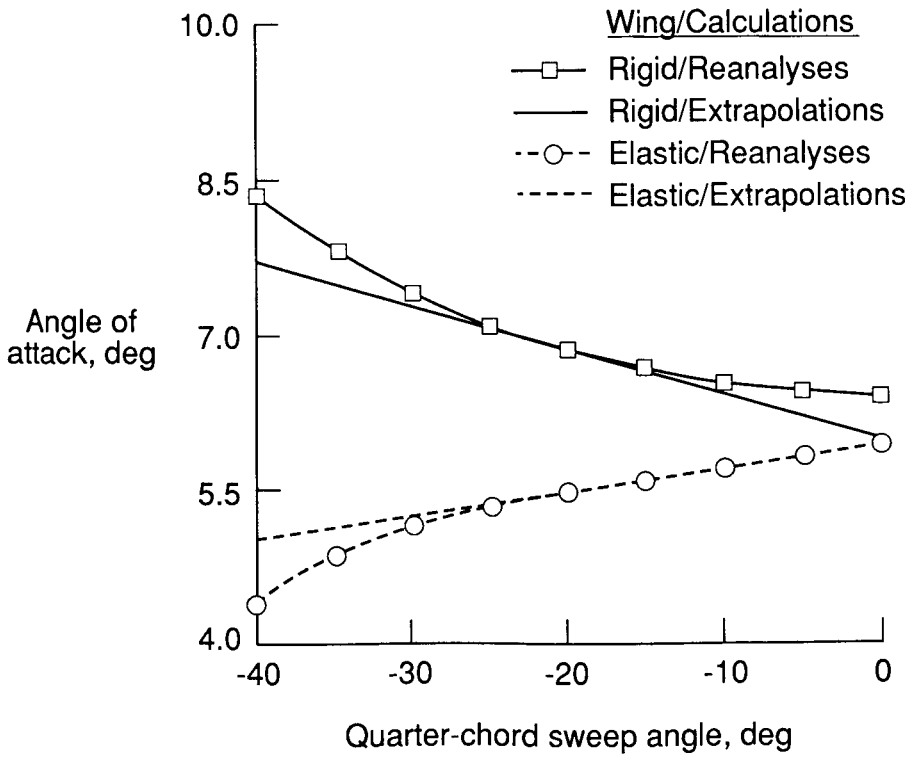

Figure 3. Sensitivity of trim angle of attack to sweep angle.

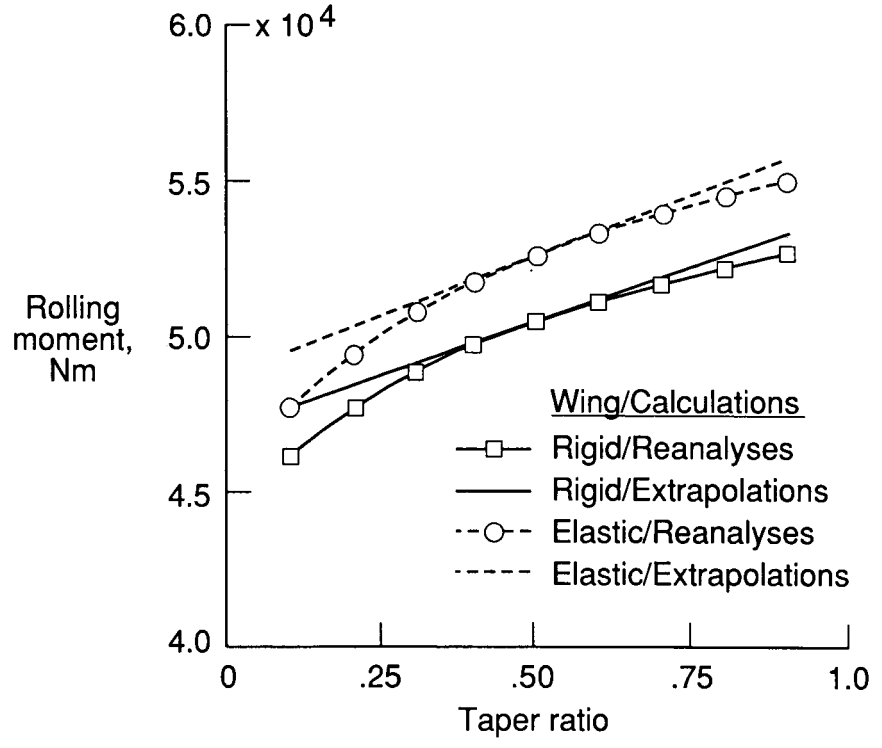

Figure 4. Sensitivity of rolling moment to taper ratio.

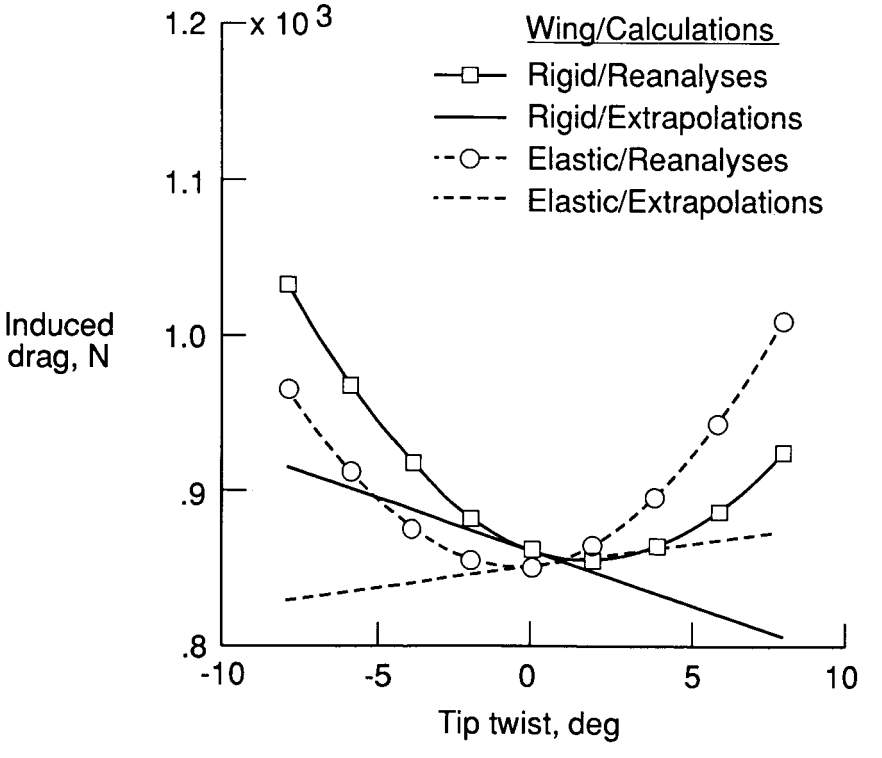

Figure 5. Sensitivity of induced drag to tip twist angle.

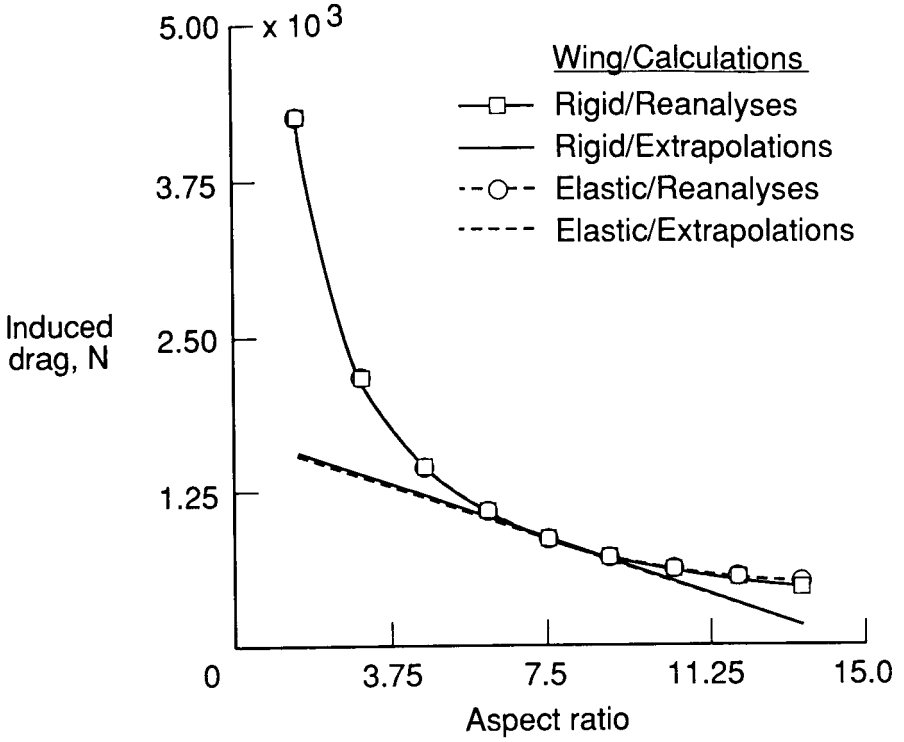

Figure 6. Sensitivity of induced drag to aspect ratio.

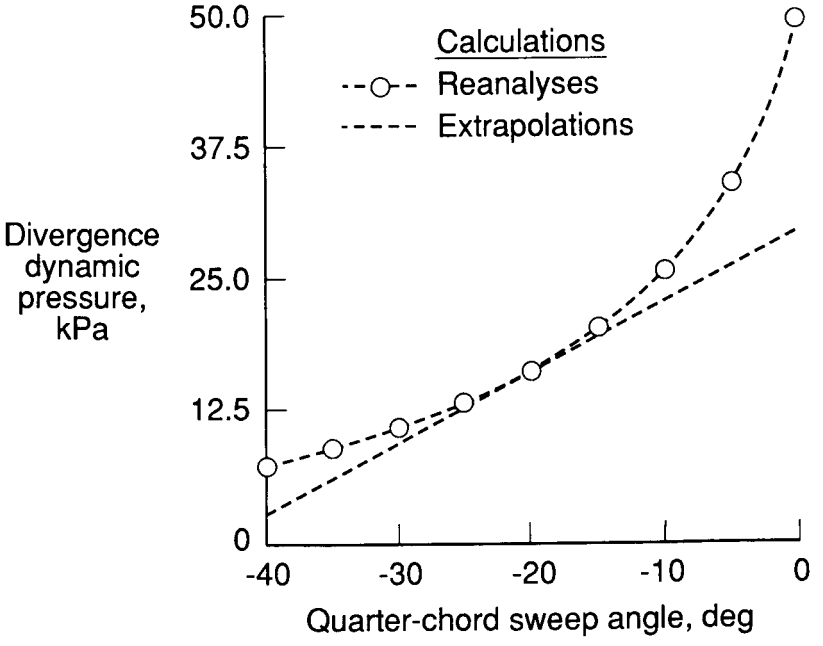

Figure 7. Sensitivity of divergence dynamic pressure to sweep angle.

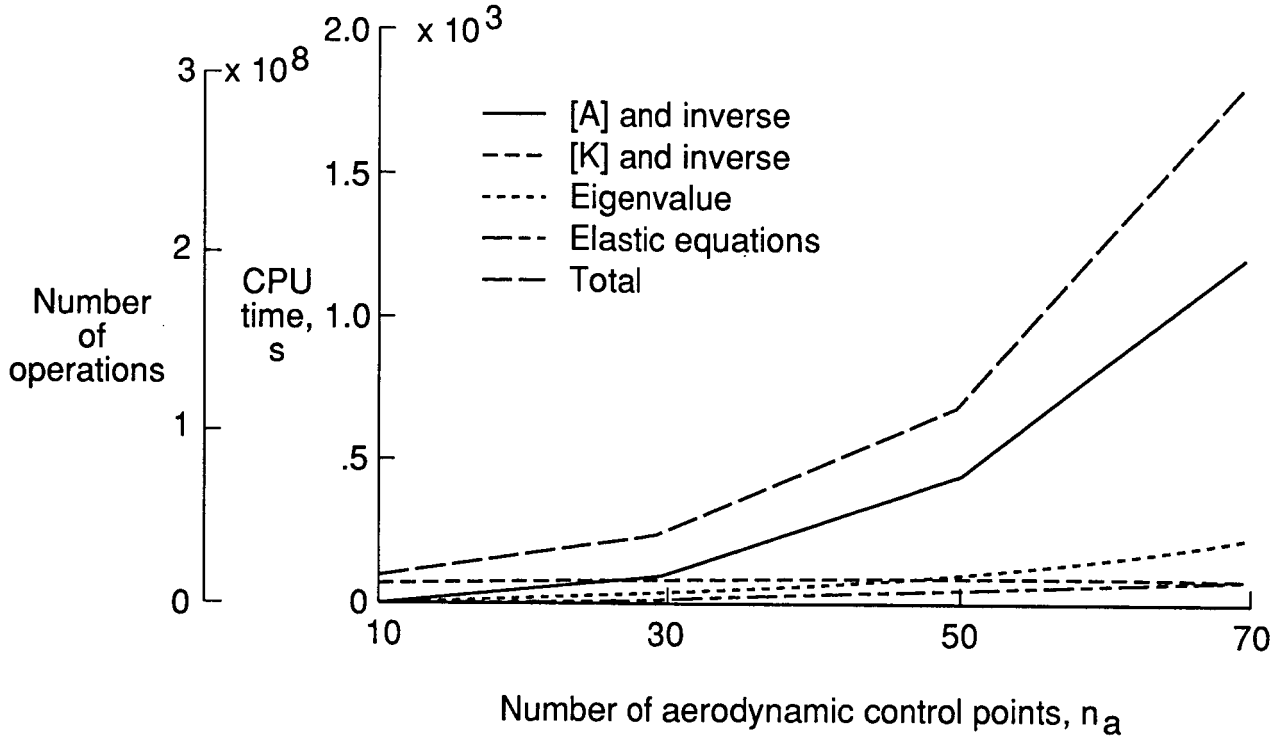

Figure 8. Cost of finite-difference sensitivity analysis.

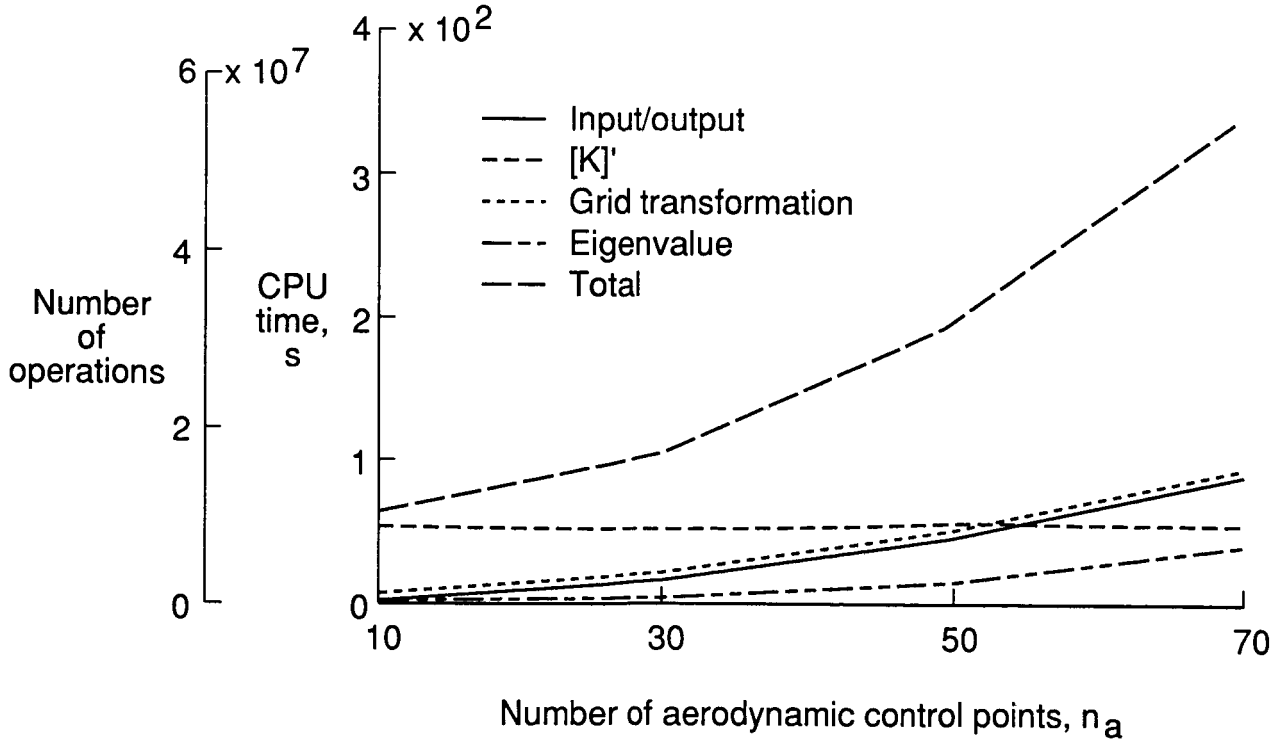

Figure 9. Cost of analytical sensitivity analysis.

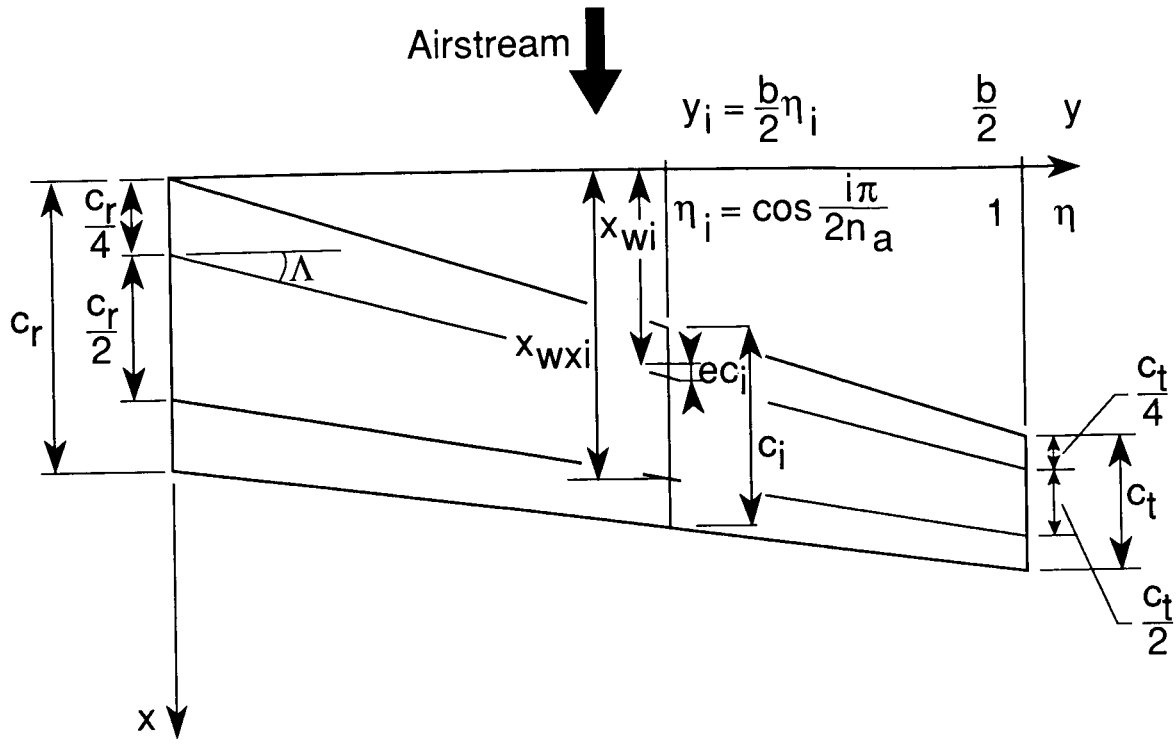

Figure 10. Geometrical definitions.

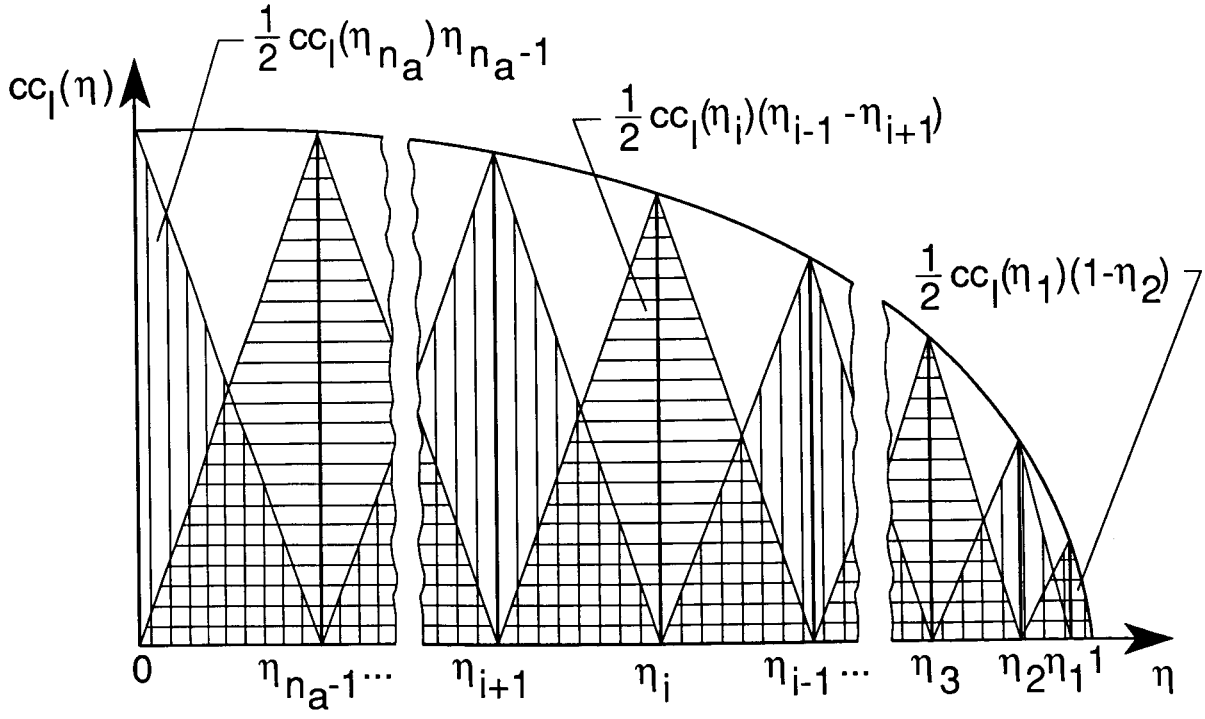

Figure 11. Spanwise load integration.

NASA
National Aeronautics and Space Administration

Report Documentation Page

1. Report No.	2. Government Accession No.	3. Recipient's Catalog No.
NASA TP-2808		

4. Title and Subtitle	5. Report Date
Shape Sensitivity Analysis of Wing Static Aeroelastic Characteristics	May 1988
	6. Performing Organization Code
7. Author(s)	8. Performing Organization Report No.
Jean-François M. Barthelemy and Fred D. Bergen	L-16418
9. Performing Organization Name and Address	10. Work Unit No.
NASA Langley Research Center Hampton, VA 23665-5225	506-43-41-01
	11. Contract or Grant No.
12. Sponsoring Agency Name and Address	13. Type of Report and Period Covered
National Aeronautics and Space Administration Washington, DC 20546-0001	Technical Paper
	14. Sponsoring Agency Code

15. Supplementary Notes

Jean-François M. Barthelemy: Langley Research Center, Hampton, Virginia.
Fred D. Bergen: Virginia Polytechnic Institute and State University, Blacksburg, Virginia.

16. Abstract

A method is presented to calculate analytically the sensitivity derivatives of wing static aeroelastic characteristics with respect to wing shape parameters. The wing aerodynamic response under fixed total load is predicted with Weissinger's L-method; its structural response is obtained with Giles' equivalent plate method. The characteristics of interest in this study include the spanwise distribution of lift, trim angle of attack, rolling and pitching moments, wing induced drag, as well as the divergence dynamic pressure. The shape parameters considered are the wing area, aspect ratio, taper ratio, sweep angle, and tip twist angle. Results of sensitivity studies indicate that (1) approximations based on analytical sensitivity derivatives can be used over wide ranges of variations of the shape parameters considered, and (2) the analytical calculation of sensitivity derivatives is significantly less expensive than the conventional finite-difference alternative.

17. Key Words (Suggested by Authors(s))	18. Distribution Statement
Shape sensitivity analysis Static aeroelasticity	Unclassified–Unlimited Subject Category 05

19. Security Classif.(of this report)	20. Security Classif.(of this page)	21. No. of Pages	22. Price
Unclassified	Unclassified	27	A03

For sale by the National Technical Information Service, Springfield, Virginia 22161-2171